UNIVERSITY OF CALIFORNIA

SANTA CRUZ

SPATIAL VARIABILITY OF SUSPENDED PARTICULATE MATTER IN SAN FRANCISCO BAY

A thesis submitted in partial satisfaction of the
requirements for the degree of

MASTER OF SCIENCE

in

OCEAN SCIENCES

by

Nicole Chin Taylor

September 2021

The Thesis of Nicole Chin Taylor
is approved:

_____
Raphael M. Kudela, Chair

_____
Sherry Palacios

_____
Claudie Beaulieu

_____
John Ryan

_____
Peter Biehl
Vice Provost and Dean of Graduate Studies

TABLE OF CONTENTS

LIST OF FIGURES AND TABLES

FIGURES

TABLES

ABSTRACT

SPATIAL VARIABILITY OF SUSPENDED PARTICULATE MATTER IN SAN FRANCISCO BAY

Nicole Chin Taylor

Understanding spatial variability of water quality in estuary systems is important for making monitoring decisions and designing sampling strategies. In San Francisco Bay, the largest estuary system on the west coast of North America, tracking the concentration of suspended materials in water is largely limited to point measurements with the assumption that each point is representative of its surrounding area. In this study, we 1) quantify spatial variability in Suspended Particulate Matter (SPM) concentrations as a proxy for water quality at different spatial scales to contextualize this assumption and 2) demonstrate the potential of satellite and shipboard remote sensing to supplement current monitoring methods. We collected radiometric data from the bow of a research vessel on three dates in 2019 corresponding to satellite overpasses by Sentinel-2. Using our ship-based data, we tracked the location of a low-salinity, high-turbidity zone to show that remote sensing of SPM can inform on physical environmental conditions. We found that features exist that are not picked up by current point sampling, which prompted us to examine how much variability exists at spatial scales between 20 m and 10 km in San Francisco Bay using 10 m resolution Sentinel-2 imagery. We found 23%-80% variability in SPM at the 5km scale (the scale at which point sampling occurs), demonstrating the risk in

assuming a single measurement is representative of a 5km area. In addition, current monitoring takes place along a transect within the Bay's main shipping channel, which we show underestimates the spatial variance of the full bay. Our results suggest that spatial structure and spatial variability in the Bay change seasonally based on freshwater inflow to the Bay, tidal state, and wind speed. We recommend monitoring programs take this into account when designing sampling strategies, and that end-users account for the inherent spatial uncertainty associated with the resolution at which data is collected. This analysis also highlights the applicability of remotely sensed data to augment traditional sampling strategies.

ACKNOWLEDGEMENTS

There are many people to thank for helping me complete this thesis. I would like to thank my advisor, Raphael Kudela, for his support and mentorship. I am grateful for the experiences working in his lab has provided, and for the countless lessons I learned working with him. Thank you to the rest of my committee – Dr. John Ryan, for his guidance and infectious enthusiasm for science; Dr. Claudie Beaulieu, for her kindness and dedication to teaching; and Dr. Sherry Palacios, for her commitment to helping students grow as people and as scientists. Thanks also to members of the Kudela Lab for their generous help and friendship. Specifically, thank you to Charlie Martin for his help with data collection, and to Meredith McPherson for her mentorship and guidance. Special thanks to Erica Nejad, Tara Schraga, Jim Cloern, and the rest of the USGS scientists who let me work with them to collect the data used in this thesis and who always made me feel welcome in their group.

I would also like to thank the Friends of Long Marine Lab Student Research and Education awards and the Earl and Ethel Myers Trust for the financial support provided to this project. I would also like to thank the NASA Student Airborne Research Program for the continued role the program has played in my scientific career.

Finally, thanks to my family and friends who supported me along the way.

CHAPTER 1

INTRODUCTION

San Francisco Bay

San Francisco Bay is the most extensive estuary system on the west coast of North America. Draining roughly 40% of California's land area (Conomos et al. 1985), the bay is a dynamic environment, with continually evolving water masses influenced both by natural processes and anthropogenic activities. The economic and societal importance of San Francisco Bay is profound: approximately 1.5 million metric tons of general cargo moves through the bay on an annual basis, and in 2019 an estimated three hundred thousand people traveled as passengers out of the port of San Francisco (sfport.com). The bay is home to eight operational bridges, numerous oil and auto ships, constant dredging operations, and a booming tourism and recreation industry, as well as a variety of unique wetland and estuarine ecosystems.

The physical environment of the bay is as dynamic as the economic system it supports. The bay itself can be simplified into three main regions: the North Bay, Central Bay, and South Bay. The Sacramento and San Joaquin rivers combine to form the San Francisco Bay Delta, which feeds into the east end of North Bay and account for 90% of the total freshwater inflow. North Bay is therefore characterized by a strong salinity gradient, starting at 0 at the mouth of the delta and increasing to 33ppt at Central Bay. This inflow of river water is the primary control on bay-wide salinity (Conomos, Smith, and Gartner 1985) and a

main source of dissolved organic carbon, nutrients, and freshwater phytoplankton to the estuarine system (Davis 1982). Freshwater input to South Bay comes from runoff and small streams, accounting for the remaining 10% of freshwater inflow. High levels of evaporation compared to precipitation increase the salinity in South Bay, which is a more static environment than its northern counterpart. Water retention time in South Bay is on the order of 3-5 months, while in North Bay water moves through as quickly as 2 weeks (Davis 1982). South and North Bay connect at Central Bay, which in turn interfaces with the Pacific Ocean.

Throughout the bay, high terrigenous influence and turbulent mixing from wind result in high levels of dissolved organic matter and suspended sediment concentrations (Davis 1982). The rivers also contribute extremely high levels of sediment and organic matter to the system (Davis 1982; Fichot and Benner 2012; Hooker et al. 2020). Suspended solid content ranges from over 250 mg/L in shallow turbid areas of South Bay to lower than 10mg/L in deeper areas of Central Bay (sfbay.wr.usgs.gov). Horizontal mixing through the bay is primarily controlled by ocean tides and freshwater inflow from the delta. Tides have a strong effect on horizontal mixing in the bay, moving water back and forth over 10's of km, but flow out of the Golden Gate is primarily controlled by the amount of freshwater inflow from the delta (Davis 1982). This freshwater inflow is strongly seasonal and links the terrestrial environment to the distribution of salinity through North Bay. In summer months, precipitation over California decreases, leading to less runoff and lower flow from the San Joaquin and

Sacramento Rivers. This allows salt water to intrude farther into the bay in the summer and fall. Conversely, in the winter and spring when precipitation is higher, the inflow from the delta increases and the salinity gradient moves westward towards San Pablo Bay (Davis 1982; Hutton, Rath, and Roy 2017). The 2ppt bottom salinity level has been defined as a metric for keeping track of these cyclic shifts in North Bay salinity, and is known as the x2 marker (Jassby et al. 1995). This virtual marker is indicative of a change in the dominant water body and is linked to the level of influence freshwater inflow has on biologic and physical aspects of the bay.

Keeping track of these intense shifts in water quality and suspended materials is a vital component in the management of San Francisco Bay. To fill this requirement, the USGS has conducted monthly monitoring cruises through San Francisco Bay since 1965. Each full-bay cruise traverses a 20 station transect starting in Redwood City and ending in Rio Vista on board the *R/V Peterson* (see figure 1, Schraga and Cloern 2017; T.S. Schraga et al. 2018). Data from these cruises are publicly available through the USGS San Francisco Bay water quality-monitoring program, and can be queried at sfbay.wr.usgs.gov.

Although the quality and length of this dataset is incredible, the USGS water quality monitoring in SFB is largely limited to point measurements, which while highly accurate, limit our ability to understand the spatial distribution of water quality in the bay. Monitoring water quality on a wide spatial scale with high continuity would be beneficial from both socio-economic and ecosystem

management perspectives. Remote sensing methods could provide this spatially comprehensive view of water quality in San Francisco Bay.

Remote Sensing in the Environment

The color of a water body is inherently linked to the materials suspended within it. Starting with the Coastal Zone Color Scanner in 1978, oceanographers have taken advantage of the relationships between quantified color and concentrations of water constituents. Passive remote sensing of biological variables, such as open-ocean chlorophyll, are commonplace and frequently used to answer questions about biogeochemical cycles and ocean ecology. However, in ocean margins, coastal processes result in complex environments with dissolved organics, multiple phytoplankton types, and various suspended particulates contributing to the overall visible signal. Pure deep water appears blue because of the scattering of short wavelengths (blue) light and the attenuation/absorption of longer wavelengths (red). Absorption and scattering of light by suspended materials influences the visible light coming off of the water, and defines the apparent color of the water body (Jerlov 1968). This visible light is quantifiable as the Remote Sensing Reflectance (R_{rs}), which is wavelength dependent and related to the total absorption and backscattering of materials in the water. This relationship is enumerated via the equation:

$$R_{rs}(\lambda) = \frac{t^2}{n^2} \frac{f}{Q(\lambda)} \frac{b_b(\lambda)}{b_b(\lambda) + a(\lambda)} \qquad (1)$$

where λ is wavelength, t is transmittance across the air-sea interface, n is the seawater index of refraction, f is the fraction of direct sunlight transmitted through the surface into the water, $Q(\lambda)$ is the ratio of upwelling irradiance to radiance, $b_b(\lambda)$ is the spectral backscatter coefficient, and $a(\lambda)$ is the total spectral absorption coefficient. The first four terms are generally treated as constant, and so the equation can be simplified to:

$$R_{rs}(\lambda) = C\frac{b_b(\lambda)}{b_b(\lambda) + a(\lambda)} \qquad (2)$$

The applications of remote sensing take advantage of the link between inherent optical properties (absorption and backscatter) to apparent optical properties such, as R_{rs}. Features of the R_{rs} spectra can inform on the scattering and absorption properties of the water, which are in turn inherently linked to particle properties. Changes in important water quality indicators—including suspended particulate matter (SPM), chlorophyll-a, and colored dissolved organic matter (CDOM)—have a direct effect on the optical properties of water. CDOM absorbs primarily blue light, appearing yellow or brown to the eye (i.e. Fichot and Benner 2012). SPM dominated by inorganic sediment scatters light strongly, and makes the apparent signal brighter in longer wavelengths at higher concentrations (Han 1997; Novoa et al. 2017). Algal particles—phytoplankton—contain a variety of absorptive colored photosynthetic pigments, the most common of which is the bright green pigment chlorophyll. CDOM, SPM, and total Chl-a serve as three baseline indicators that characterize the water quality of a particular area,

informing on the concentration of dissolved carbon, inorganic particles, and productivity of a water mass. These indicators serve as proxies for other biogeochemical variables that cannot be directly measured using passive remote sensing (i.e. Fichot et al. 2016; Fichot and Benner 2012; Hilton et al. 2018). Changes in these indicators are thus discernable in the visible R_{rs} spectra and quantifiable with multi-spectral visible imaging spectroscopy (i.e. Dierssen et al. 2006; Fichot et al. 2016; Nechad, Ruddick, and Park 2010). Traditional remote sensing methods are most useful in optically simple environments, where one component dominates the visible signal and other constituents are relatively low-concentration and co-varying (www.oceanopticsbook.info). Optically complex environments, like coastal oceans and San Francisco Bay, have optically active components that do not always co-vary, resulting in a more complex and nuanced total signal. New technologies present opportunities for improving retrievals of biophysical variables from remote sensing data in complex coastal environments. The advent of hyperspectral sensors provides increased spectral information available for remote sensing algorithms to use. Hyperspectral sensors have the advantage over multi-spectral sensors in that they provide much higher spectral resolution, rather than just a few bands.

Understanding spatial variability and water quality patterns in the San Francisco Bay environment could advance monitoring efforts and elevate our understanding of the estuary. Traditional remote sensing is underutilized in San Francisco Bay because: 1) high levels of sediment, algae, and other material result

in complicated signals (Mao et al. 2010), and 2) high spatial variability across small length scales make coarse (>200m) resolution problematic (Davis et al. 2007; Moses et al. 2016), and 3) the dense fog often masks the Bay Area. In this thesis address we use the USGS *R/V Peterson* as a remote sensing platform and combine data with high resolution multispectral data from Sentinel 2 to examine spatial variability of SPM in San Francisco Bay.

References

Conomos, T. J., R. E. Smith, and J. W. Gartner. 1985. "Environmental Setting of San Francisco Bay." *Hydrobiologia* 129(1): 1–12.

Di Cicco, Annalisa et al. 2017. "Obtaining Phytoplankton Diversity from Ocean Color: A Scientific Roadmap for Future Development." *Frontiers in Marine Science*.

Davis, Curtiss O. 1982. "The San Francisco Bay Ecosystem - A Retrospective Overview." In *San Francisco Bay Use and Protection*, eds. William J. Kockelman, T. John Conomos, and Alan E. Leviton. Pacific Division: American Association for the Advancement of Science, 17–37.

Dierssen, Heidi M., Raphael M. Kudela, John P. Ryan, and Richard C. Zimmerman. 2006. "Red and Black Tides: Quantitative Analysis of Water-Leaving Radiance and Perceived Color for Phytoplankton, Colored Dissolved Organic Matter, and Suspended Sediments." *Limnology and Oceanography* 51(6): 2646–59. http://doi.wiley.com/10.4319/lo.2006.51.6.2646.

Fichot, Cédric G. et al. 2016. "High-Resolution Remote Sensing of Water Quality in the San Francisco Bay-Delta Estuary." *Environmental Science and Technology* 50(2): 573–83.

Fichot, Cédric G., and Ronald Benner. 2012. " The Spectral Slope Coefficient of Chromophoric Dissolved Organic Matter (S 275-295) as a Tracer of Terrigenous Dissolved Organic Carbon in River-Influenced Ocean Margins ." *Limnology and Oceanography* 57(5): 1453–66.

Han, Luoheng. 1997. "Spectral Reflectance with Varying Suspended Sediment Concentrations in Clear and Algae-Laden Waters." *Photogrammetric Engineering and Remote Sensing* 63(6): 701–5.

Hilton, Annette E., Jesse T. Bausell, and Raphael M. Kudela. 2018. "Quantification of Polychlorinated Biphenyl (PCB) Concentration in San Francisco Bay Using Satellite Imagery." *Remote Sensing* 10(7): 1–18.

Hooker, Stanford B. et al. 2020. "A Global End-Member Approach to Derive CDOM (440) from near-Surface Optical Measurements." *Biogeosciences* 17(2): 475–97.

Hutton, Paul H., John S. Rath, and Sujoy B. Roy. 2017. "Freshwater Flow to the San Francisco Bay-Delta Estuary over Nine Decades (Part 2): Change Attribution." *Hydrological Processes* 31(14): 2516–29.

Jassby, A. D. et al. 1995. "Isohaline Position as a Habitat Indicator for Estuarine Populations." *Ecological Applications* 5(1): 272–89.

Jerlov, N.G. 1968. *Optical Oceanography*. Volume 5. Elsevier. https://linkinghub.elsevier.com/retrieve/pii/S0422989408709176.

Mao, Zhihua et al. 2010. “Effects of Phytoplankton Species Composition on Absorption Spectra and Modeled Hyperspectral Reflectance.” *Ecological Informatics*.

Mobley, Curtis D. et al. 2005. “Interpretation of Hyperspectral Remote-Sensing Imagery by Spectrum Matching and Look-up Tables.” *Applied Optics*.

Moses, Wesley J. et al. 2016. “Spatial Scales of Optical Variability in the Coastal Ocean: Implications for Remote Sensing and in Situ Sampling.” *Journal of Geophysical Research: Oceans* 121(6): 1–15. http://doi.wiley.com/10.1002/2016JC011767.

Mouw, Colleen B. et al. 2017. “A Consumer’s Guide to Satellite Remote Sensing of Multiple Phytoplankton Groups in the Global Ocean.” *Frontiers in Marine Science* 4(February).

Nechad, B., K. G. Ruddick, and Y. Park. 2010. “Calibration and Validation of a Generic Multisensor Algorithm for Mapping of Total Suspended Matter in Turbid Waters.” *Remote Sensing of Environment* 114(4): 854–66. http://dx.doi.org/10.1016/j.rse.2009.11.022.

Novoa, Stéfani et al. 2017. “Atmospheric Corrections and Multi-Conditional Algorithm for Multi-Sensor Remote Sensing of Suspended Particulate Matter in Low-to-High Turbidity Levels Coastal Waters.” *Remote Sensing* 9(1).

Palacios, Sherry L. et al. 2015. “Remote Sensing of Phytoplankton Functional Types in the Coastal Ocean from the HyspIRI Preparatory Flight Campaign.” *Remote Sensing of Environment*.

Roberts, D. A. et al. 1998. “Mapping Chaparral in the Santa Monica Mountains Using Multiple Endmember Spectral Mixture Models.” *Remote Sensing of Environment* 65(3): 267–79.

Schraga, T.S., E.S. Nejad, C.A. Martin, and J.E. Cloern. 2018. *USGS Measurements of Water Quality in San Francisco Bay (CA), Beginning in 2016 (Ver. 2.0, June 2018)*. Menlo Park. https://sfbay.wr.usgs.gov/access/wqdata/index.html.

Schraga, Tara S., and James E. Cloern. 2017. “Water Quality Measurements in San Francisco Bay by the U.S. Geological Survey, 1969-2015.” *Scientific Data* 4: 1–14.

Xi, Hongyan, Martin Hieronymi, Hajo Krasemann, and Rüdiger Röttgers. 2017. “Phytoplankton Group Identification Using Simulated and in Situ Hyperspectral Remote Sensing Reflectance.” *Frontiers in Marine Science* 4(AUG): 1–13.

CHAPTER 2

SPATIAL VARIABILITY OF SUSPENDED PARTICULATE MATTER IN SAN FRANCISCO BAY

INTRODUCTION

San Francisco (SF) Bay is the most extensive estuary system on the west coast of North America, draining roughly 40% of California's land area into the Pacific Ocean (Conomos et al. 1985). The bay is home to over 500 species of birds, fish, and other wildlife: it is an important feeding area and wintering ground for migrating birds, and two-thirds of California's salmon migrate through SF Bay annually. In addition to the wildlife it supports, the surround Bay Area is home to over 7 million people and supports important tourism, technology, and agricultural economies. The bay is home to eight operational bridges, numerous oil and auto ships, constant dredging operations, a booming tourism and recreation industry, and a variety of unique wetland and estuarine ecosystems.

The Bay itself is a shallow wetland system, with most of the bay less than 6 m deep. The exception is a shipping channel which runs through the middle of the Bay (Figure 1). This shipping channel is the deepest part of the Bay with depths greater than 10 m and is dredged regularly to facilitate the movement of ship traffic. This stark difference in bathymetry and higher flow velocities in the shipping channel (Bever and MacWilliams 2013) make it distinctive from the rest of the Bay.

SF Bay can be simplified into three main regions: the North Bay, Central Bay, and South Bay (Figure 1). These regions can be approximately defined by the location of bridges crossing the Bay: North Bay is the region of the Bay north of the Richmond Bridge, Central Bay is the region between the Richmond and Bay Bridges, and South Bay is the region south of the Bay Bridge. These regions each experience different physical processes driving water movement and spatial variability.

The full SF Bay is connected to two major water bodies: the San Francisco Bay Delta in the Northeast, and the Pacific Ocean in the West. The San Francisco Bay Delta feeds into east North Bay and is where the Sacramento and San Joaquin rivers combine. Inflow from the Delta accounts for 90% of the total freshwater inflow to the Bay. North Bay is therefore characterized by a strong salinity gradient, starting at 0 at the mouth of the delta and increasing to 33ppt at Central Bay. This inflow of river water is the primary control on bay-wide salinity (Conomos, Smith, and Gartner 1985) and the primary source of suspended sediments, nutrients, and freshwater phytoplankton to the estuarine system (Davis 1982). The remaining 10% of inflow to the Bay comes from runoff and other point sources.

Flow out of SF Bay is primarily controlled by the amount of freshwater inflow from the Delta (Davis 1982). The Bay drains into the Pacific Ocean through the Golden Gate (Figure 1). The Pacific Ocean exerts strong tidal influence on horizontal mixing SF Bay, moving water back and forth over 10's of km. The

combination of inflow from the Delta, tidal mixing from the Pacific, varied bathymetry, and wind-driven mixing creates a highly dynamic system. Each type of physical forcing has different levels of influence on North, Central, and South Bay: for example, the strong salinity gradient set up by Delta flow in North Bay creates a very different environment than South Bay. Water retention time in South Bay is on the order of 3-5 months, while in North Bay water moves through as quickly as 2 weeks (Davis 1982).

The spatial distribution of Suspended Particulate Matter (SPM) is tied to physical mixing dynamics in SF Bay. The Delta is the main source of SPM into the Bay (Powell et al. 1989), SPM moves with tidal pumping (Ganju et al. 2004), and wind-driven resuspension over different bathymetry drives localized SPM concentrations (Schoellhamer 2011, Bever et al. 2018). SPM can also be used as a proxy for a variety of water quality applications: SPM concentrations are linked to other environmental conditions in SF Bay, including flow velocities, salinity (Schoellhamer 2000), anthropogenic pollutants (Hilton et al. 2018), Methylmercury (Fichot et al. 2016), nutrients, and light availability. Therefore, understanding spatial distributions and patterns in SPM informs on other environmental conditions.

Keeping track of SPM and other water quality metrics is currently done via point monitoring and regular sampling. The USGS Water Quality Monitoring Program has conducted monthly monitoring cruises through San Francisco Bay since 1964. Each full-bay cruise traverses a 20 station transect starting in

Redwood City and ending in Rio Vista onboard the *R/V Peterson* (Figure 1, Schraga and Cloern 2017; T.S. Schraga et al. 2018). These monitoring stations are strategically set up to track mean bay-wide conditions, but not to capture spatial variability in water quality properties (Jassby et al. 1997). The transect is also conducted exclusively in the shipping channel, which is distinctive from the rest of the Bay because it is deeper and has higher flow velocities (Bever and MacWilliams 2013). Localized studies supplement bay-wide monitoring with higher-resolution information on specific inflow points around SF Bay (i.e. Morgan-King and Schoellhamer 2013). However, as SF Bay undergoes continuous change and restoration, expanding monitoring efforts to be more spatially resolved is becoming more important.

One way to expand monitoring efforts is with remote sensing, which provides broad spatial coverage and the ability to collect a large amount of data regularly. Remote sensing has provided a coarse overview of SPM concentrations in the Bay (Ruhl et al. 2001), but in general has been underutilized in SF Bay because of high spatial variability and comparatively low sensor resolution. The advent of high-resolution remote sensing technology and satellite imagery has expanded the potential for remote sensing of sediments in SF Bay. In recent years, remote sensing technology has advanced and made remote sensing of SF Bay in high-resolution possible. Notably, Fichot et al. (2016) used the JPL PRISM sensor to map turbidity and water quality at high (2 m) resolution in a northern area of SF Bay (Grizzly Bay). Although flying high-altitude aircraft is a logistically

difficult way to regularly monitor water quality, surface-level sensors are becoming smaller and more feasible for regular deployment onboard ships (e.g. the Ferry Ocean Colour Observation Systems (FOCOS) project, Brando et al. 2015), and provide data at similar resolution to airborne systems. In addition, the launch of higher resolution sensors like the European Space Agency's 10m resolution MultiSpectral Instrument (MSI) onboard the Sentinel-2 satellite provide imagery capable of resolving small-scale features across the entire bay.

These new high-resolution satellite sensors and new ship-based systems can help expand monitoring efforts in two ways: 1) by being an additional data source, and 2) by providing more spatial information for making sampling decisions. Our study has two main goals. The first goal is to compare shipboard and satellite remote sensing of SPM in SF Bay to examine how each data type contributes to monitoring in terms of accuracy and spatial coverage. The second goal is to quantify spatial variability of SPM in SF Bay using remote sensing, to contextualize sampling strategies and future monitoring. Specifically, we use remote sensing of SPM to address the question: How much spatial variability exists at different spatial scales in SF Bay, and how much is captured by monitoring at different resolutions? Overall, this project seeks to provide information on 1) how remote sensing can directly contribute to monitoring water quality in SF Bay, and 2) the overall variability that exists at different scales in the Bay.

METHODS

Data collection and data types

To examine how remote sensing methods can supplement existing in-water monitoring methods, we collected four types of data in collaboration with the USGS Water Quality Monitoring Program. We used *in situ* SPM grab sample measurements and continuous turbidity flow-through data taken by the USGS as part of their standard monitoring procedure; continuous radiometric data taken from the bow of the USGS research vessel, the *R/V Peterson*; and 10 m satellite imagery from the MultiSpectral Imager onboard the European Space Agency's Sentinel-2 satellite. In sum, we are using discrete SPM grab samples, continuous flow-through and shipboard radiometry taken along a transect, and spatially complete satellite imagery covering the full bay.

The ground-based data used in this study were collected on April 25, June 4, and October 23, 2019 onboard the *Peterson*. Each cruise began at approximately 6:00am local time (PDT) from Redwood City harbor and ended between 3-5:00pm in Antioch (Figure 1). Sentinel-2 imagery was always acquired at 11:30am PDT. Sentinel-2 overpasses occurred on both the April and June dates. No Sentinel overpasses occurred on October 23, so instead we used imagery that was collected on October 22. Because the October overpass occurred on a different day than the cruise, we did not directly compare ship and satellite data for October.

Discrete *in situ* grab samples

Water quality measurements including SPM concentration (mg/L) were collected at regular point stations (Figure 1) at 2m depth, according to USGS standard operating procedures. Quality controlled data from the USGS are available for public use (sfbay.wr.usgs.gov).

Continuous Flow-through Data

Continuous underway measurements of turbidity were collected every 5 seconds at 2 meters depth throughout each cruise using a Self-Contained Underwater Fluorescence Apparatus (SCUFA). These underway flow-through data were validated following the standard operating procedure of the USGS San Francisco Bay Water Quality Monitoring program (Schraga et al. 2020). To summarize, data were filtered using a low-pass filter with a 60 second corner frequency to remove bubble noise in the system. Flow-through data taken while the ship was sampling at designated stations (Figure 1) were averaged and compared to corresponding discrete samples using linear regression. If the regression line had an $R^2 > 0.7$, the relationship was accepted and used to convert all the filtered flow-through data to SPM units. If the R^2 was less than 0.7, the data was geographically split into groups of at least three points. A new regression was fit for each group and used to convert flow-through data contained in each group to SPM.

Continuous Shipboard Radiometry Data

In addition to the regular USGS data, a HOBI Labs HydroRad-3 (HydroRad) hyperspectral radiometer was mounted at the ship's bow and set to record continuously throughout each cruise. Discrete hyperspectral measurements from an Analytical Spectral Device (ASD) FieldSpec HandHeld 2 Spectroradiometer were also taken to corroborate HydroRad data at locations corresponding to simultaneous water quality measurements. Prior to being deployed, the data quality and signal to noise ratio of the HydroRad were checked against the ASD in stable conditions.

Onboard the *R/V Peterson*, the HydroRad recorded continuous radiometry measurements of downwelling irradiance (E_d), sky radiance (L_{sky}), and total radiance from the water (L_T). Care was taken throughout the cruise to keep the HydroRad's sensors pointing 100˚-130˚ from the sun. The HydroRad's three sensors were fixed 2 m above the main deck on the ship bow. L_T was fixed 40˚ down from horizontal, L_d was fixed 40˚ up from horizontal, and E_d was fixed straight up.

HydroRad data collected before station 18 were removed to eliminate data taken in low-light conditions (i.e., solar elevation below 30˚). The remaining data were processed following Mobley (1999). Remote sensing reflectance was calculated from the HydroRad data using the equation:

$$R_{rs}(\lambda) = \frac{L_T(\lambda) - \rho_{sky} L_{sky}(\lambda)}{E_d(\lambda)} \qquad (1)$$

Where λ is wavelength, and $\rho_{sky} = 0.1$ to correct for skylight reflectance off the water surface (Austin 1974, Mobley 1999). Data were inspected for quality control and manually compared to ASD measurements. Flat spectra and spectra with negative values were removed, and a running 10-point median filter was applied to remove high frequency noise (attributed to glint) from the remaining data. The total number of data points were N = 1,398, N = 1,995, and N = 849 for April, June, and October, respectively. The average distance between R_{rs} data points depended on the sensor's automatic integration time and light conditions, and was 79 m, 95 m, and 113 m for each of the three cruises.

SPM was calculated from HydroRad R_{rs} along each cruise track using the algorithm developed by Nechad et al. (2010), which was chosen because it has been shown to work well in this region (Hilton et al. 2018). This algorithm uses a single channel to determine SPM based on spectral brightness, and then uses an empirically derived set of coefficients to calculate SPM. We chose to synthesize a band centered at 700 nm by averaging all hyperspectral channels within an 8 nm window. 700 nm was deemed appropriate based on the recommendations in Nechad et al. (2010), preliminary tests, and an observed increase in sensor noise above 700 nm. Retrieved SPM values from data taken at stations were compared to validated flow-through SPM for each cruise (Figure 2).

Satellite Processing

To examine SPM outside the shipping channel, we use imagery from Sentinel-2 overpasses on April 25, June 4, and October 22, 2019. Concurrent USGS cruises with radiometry occurred on April 25, and June 4. No ground data were collected on October 22 but were collected on October 23. A 1-day difference is outside the temporal window for comparison in SF Bay (Hilton et al. 2018). Consequently, direct comparisons between ground and satellite data are only made for April and June, and the October data were simply used as a sanity check.

For each date, two images of SF Bay were acquired immediately after each other at approximately 11:30am PDT. Imagery was downloaded from the ESA open-access data portal (scihub.copernicus.eu) in two different versions; one set processed to Level 2A standard reflectance, and a second set processed to Level 1C standard normalized water-leaving radiance.

Images were mosaicked using the ESA's open-source imaging processing software, SNAP, to create a full Level 2A reflectance image and a full Level 1C radiance image for each date. No imagery was available for the Delta region encompassing station 657 for any date as it is outside of the satellite footprint.

The Nechad et al. (2010) SPM algorithm was applied to the Level 2A reflectance image to retrieve SPM concentrations for the full bay. However, April and June images displayed a false elevation of SPM in the Central Bay region near station 18 and in the Sacramento River near stations 3 and 649 (Figure 2) when compared to *in situ* data. This could be due to inaccuracies in the standard

atmospheric correction over water. We therefore tried using a different processing strategy: we tested using the Case 2 Regional CoastColour (CR2CC) processor in SNAP with Level 1C radiance imagery. The CR2CC processor uses a set of neural networks to match observed conditions with a library of radiative transfer simulations representative of different water types (Brockmann et al. 2016). It has been specifically developed to work with certain satellite sensors and takes atmospheric conditions into account and is available to use in SNAP. CR2CC does a simultaneous atmospheric correction and SPM retrieval.

We compared the reflectance from Sentinel-2 processed with C2RCC, the reflectance from the standard Level 2A Sentinel-2 product, and the reflectance taken by the HydroRad in Figure (Figure 3). We also compared the SPM results from CR2CC, the SPM results from Nechad and the standard Level 2A reflectance product, SPM from the HydroRad, and *in situ* data (Figure 3). The C2RCC results matched both the HydroRad reflectance and the *in situ* SPM data better than the Level 2A with Nechad algorithm, and so we used the C2RCC results for the rest of our analysis.

Spatial Variability Analysis

We examine spatial variability using the SPM distribution maps created from Sentinel-2 imagery using the Coefficient of Variance (CV) method outlined by Moses et al. (2016). This analysis defines the amount of spatial variability at different scales. The method is similar to a semi-variogram or spatial

autocorrelation, but we chose this method over others because it is mathematically similar to an inverted Signal to Noise Ratio or uncertainty metric. This allows us to think of the CV as a measure of how representative a single sample is for an area. As larger and larger areas are considered, the variability increases rapidly at small scales first and then more slowly at larger scales, following a logarithmic relationship.

The amount of spatial variability is calculated as a function of increasing distance or area (Ground Sampling Distance, GSD). Spatial variability was quantified as the Coefficient of Variance (CV, Moses et al. 2016), defined as

$$CV_x = \frac{1}{n}\sum_{i=1}^{n}\left(1+\frac{1}{4k}\right)\frac{\sigma_i}{\overline{x_i}} \qquad (2)$$

where n is the number of segments the dataset is broken into, k is the number of data points in each segment, x_i is the within-segment mean, and σ_i is the within-segment bias-corrected standard deviation. The CV is essentially a measure of how representative a single measurement is for a region defined by GSD.

The rate at which variability is gained with distance can be quantified as *dCV/dGSD*. We modeled the relationships between CV and GSD for each dataset using a logarithmic function (Moses et al. 2016). The transition point where this rate changes (GSD_T) represents the sampling distance at which variability begins to increase more slowly. Moses et al. used two different methods for finding the transition GSD: the first was the find a log-log intersect, and the second was to identify the GSD where slopes reached the 66th percentile. Our data didn't display

any clear log-log intersect, and the 66th percentile method was arbitrary and did not transfer to our study. Instead, we defined the GSD_T as the GSD where $dCV_x/dGSD = 1x10^{-4}$, i.e. where the slope transitioned through 1% CV per 100m. This gives us a fixed metric to compare across our datasets and represents a clear transition point in $dCV_x/dGSD$.

We conducted three distinct SPM spatial variability comparisons. First, we calculated the CV/GSD relationship for the full Bay on each date to examine how variability changed between months. Second, we compared those full Bay relationships with variability in just the shipping channel. This was done by extracting just SPM values along the USGS cruise transect. The analysis was repeated using just the data that lie within the shipping channel. Third, we examined the variability in different regions of the Bay by repeating the analysis for the North, Central, and South Bay regions.

Environment Conditions

We obtained Delta flow data from the California Natural Resources Agency's Dayflow dataset, which is a computer program used for tracking historical mean daily flows into SF Bay from the Delta (data.cnra.ca.gov/dataset/dayflow). Information on tidal phase and state is from NOAA's Tides and Currents Water Level product for SF Bay (tidesandcurrents.noaa.gov). Wind data were taken *in situ* at each station as part of the radiometry data collection protocol. At the time of each satellite overpass,

wind was measured at 7.7 m/s, 0.5 m/s, and 1.3 m/s at USGS station 13, which is where the *R/V Peterson* was sampling at the time.

Tidal conditions on each date were as follows. In April, SF Bay was switching from spring to neap tide conditions, and imagery was taken at a peak high tide of 1.6 m. The June image was taken at the height of spring tide, during a falling tide at 0.6 ft with the tide going out at time of satellite overpass. In October conditions were switching from spring to neap tide, and it was a falling tide at 0.6 ft with tide going out at time of satellite overpass. All imagery was taken at 11:30 am PDT.

Delta flow on each date followed seasonal patterns. The inflow from the Delta was similar for April and June (rainy season), then much lower in October (dry season). Delta inflow in April was 68,464 cfs (cubic feet per second) and in June was 66,005 cfs. The April cruise occurred following peak flooding and the June cruise occurred at a local peak in delta flow (relatively smaller flood event). In October, Delta inflow dropped by a factor of four to 15,845 cfs.

RESULTS

Shipboard Radiometry vs. *in situ* Flow-through SPM

The relationship between retrieved SPM from the HydroRad and *in situ* SPM from the flow-through system was highly correlated ($R^2 \geq 0.49$) on each cruise. This correlation stayed near a 1:1 relationship but differed from cruise to cruise. HydroRad SPM underestimated the flow-through SPM (slope = 2.15) in

April but were more aligned in June and October (slopes of 1.08 and 0.87, respectively). The steep slope in the April data could be due to high stratification between the *in situ* grab samples at 2m depth and the surface SPM concentration retrieved by the shipboard HydroRad data, but this is unconfirmed.

The full transects of HydroRad SPM, flow-through SPM, and in situ grab samples are compared in Figure 3. The average distance of grab sample measurements is 8 km, and the average distance between HydroRad measurements was 95.8 m, excluding repeats taken when the boat was paused at stations. Notably, the turbidity maximum can be identified in all datasets but is better resolved in the HydroRad data. The central peak and eastern side of the turbidity maximum corresponds with the location and slope of the salinity gradient. In April the turbidity and salinity transition point are mid-way in the Carquinez Strait near station 9; in June, both features are present just west of station 9; and in October, the transition point moves eastward into the Sacramento River near station 3.

Smaller notable features also occur in the transects. A significant peak occurs near station 9 for all dates, although the exact location of the peak shifts slightly. This persistent turbidity feature in the Carquinez straight is not captured by the grab sample stations. The magnitude of this feature changes, from around 40 mg/L in April, up to 120 mg/L in June, and down to 15 mg/L in October. This feature can also be seen in the satellite imagery from each date as tongue of

elevated SPM reaching down from Grizzly Bay into the Carquinez straight (Figure 6).

Satellite Radiometry vs Shipboard Radiometry

The standard Sentinel-2 Level 2A reflectance overestimates the spectral brightness compared to the HydroRad spectra. The Sentinel-2 C2RCC spectra match the HydroRad spectra more closely. Figure 3 shows the comparison of the standard Level 2A and the C2RCC Sentinel-2 spectra against the HydroRad spectra at the stations closest in time to the Sentinel-2 overpass.

Satellite SPM results

C2RCC provided the most accurate SPM retrievals with the Sentinel-2 data, and was used to generate maps of SPM on April 25, June 4, and October 22. General statistics for each date are presented in Table 1. April and June displayed high concentrations of SPM, with mean values of 46.25 mg/L and 47.78 mg/L respectively. In contrast, October had a mean value of 9.06 mg/L. The range for each date was 149.58 mg/L, 148.83 mg/L, and 46.21 mg/L for April, June, and October respectively. Lower South Bay and upper San Pablo Bay consistently had the highest SPM. Central Bay had the lowest SPM values—in June and October the lowest SPM values are at the Golden Gate, but in April that section of SF Bay was blocked by clouds. Other prevalent spatial patterns included low SPM values

in the northern section of the shipping channel in April and June, and consistent filamented structure in the middle of South Bay.

Differences in SPM and spatial structure on each date are apparent. Worth noting is the widening of the low-SPM area in the shipping channel through San Pablo Bay in the June image compared to the April image. Changes in SPM along the Delta to North Bay gradient through Grizzly Bay occur as the system shifts from high Delta flow conditions (April and June) to low Delta flow (October). Closer inspection of the Carquinez straight and Grizzly Bay also elucidates the structure of the Carquinez straight feature observed in the transect data: a filament of high SPM runs along the northwestern shore of Grizzly Bay and intrudes into the shipping channel cruise track. This pattern is most pronounced in the June image. The high-SPM filament moves from the shore in April/June to the middle of the channel in October.

Spatial Variability Analysis

To quantify how much variability exists at different spatial scales in SF Bay, we calculated the relationship between spatial scales defined by the Ground Sampling Distance (GSD) and variability defined by the Coefficient of Variance (CV). For all datasets, the relationship between GSD and CV followed the logarithmic relationship described by Moses et al. (2016). We considered the modeled CV as a measure of how representative a single measurement is of a

surrounding area of size GSD. The rate of change, *dGSD/dCV*, was consistently positive for all datasets.

We talk specifically about two metrics: the Transition GSD (GSD_T); and the CV at a GSD of 5 km (CV_{5km}). The GSD_T is the inflection point where *dGSD/dCV* switches from rapidly increasing to slowly increasing and indicates the scale (GSD) at which variability begins to level off. The CV_{5km} is the CV at the 5 km scale, which is the approximate scale of USGS point sampling in the Bay.

Comparison Between Dates

April had the most variability across all scales (GSDs) of all the dates. Specifically, the CV_{5km} decreased 20% from April to June and October (full area CV_{5km} of 51%, 32%, 32%). June and October had much more similar variability with CV_{5km} of 32% for both dates. This is also reflected in the GSD_T metric for each date: April, June, and October respectively had GSD_T values of 921 m, 461 m, and 421 m, indicating much more heterogeneous conditions in April than the other two months.

This pattern of heterogeneity was not reflected in the shipping channel-only analysis. Although April still had the highest variability, June and October had different levels of variability within the shipping channel. CV_{5km} within the shipping channel was 20%, 16%, and 12% for April, June, and October respectively.

Comparing the shipping channel to the full area of SF Bay, we found that on average there is approximately twice the amount of variability in the full area than just the shipping channel transect. This approximate doubling of variability is consistent across different regions and dates but does change with scale. At smaller scales (i.e. 100m), the ratio of area variability to transect variability is about 1.5, but above a 1 km scale the ratio is about 2.

Regional Comparison

For all dates, Central Bay had the highest CV at all GSDs, followed by South Bay, and North Bay had the lowest CVs. Specifically considering the average across all dates, North, Central, and South Bay had an average CV_{5km} of 30%, 53%, and 43% respectively. At a smaller scale of GSD = 100 m, North, Central, and South Bay each had an average CV of 10%, 18%, 13% compared to an average full bay CV of 12%. The *dGSD/dCV* for South Bay was lower than other regions of SF Bay (illustrated by slower increase in CV/GSD relationship, Figure 5), implying less small-scale variability. Variability conditions in Central and South Bay were also more inconsistent than North Bay: between all dates at GSD = 10 km, the CV of Central Bay ranged 32%-89%, South Bay ranged is 32%-81%, and North Bay ranged 33%-37%. This indicates that North Bay has the most consistent CV/GSD relationship and spatial structure of the three regions.

The GSD_T values for each region (Table 2) also indicate that North Bay has less spatial variability than Central and South. The GSD_T represents the scale at

which spatial patterns begin to become more homogenous and indicates dominant physical mixing processes. A larger GSD_T corresponds to more spatial variability in the environment, and a lower GSD_T corresponds to less spatial variability. The average GSD_T for each region was 451 m, 894 m, and 698 m for North, Central, and South Bays respectively, and 601 m for the full bay. A similar but less pronounced pattern is represented in the transect GSD_T values of 118 m, 138 m, and 174 m for North, Central, and South Bays and 161 m for the full bay. Notably, the GSD_T of the shipping channel transect through a region on a specific date does not necessarily represent the corresponding GSD_T of the fully resolved area. For example, in June, South Bay has the highest GSD_T for both the transect and areas, and North Bay has the lowest. However, in October, the transect GSD_T suggest Central Bay is more small-scale dominated than North or South Bay, but the area GSD_T suggests that Central Bay has more variability than the other two regions.

DISCUSSION

The objectives of this study were to 1) examine the ways in which remote sensing data could provide increased spatial coverage for monitoring programs in SF Bay, and 2) to quantify the amount of spatial variability that exists at different spatial scales in the Bay. Our results show that remote sensing data provide higher spatial coverage at the cost of accuracy: continuous SPM retrievals taken along a transect are slightly less accurate than discrete SPM samples, and both are more

accurate than satellite SPM retrievals. We also found that continuous SPM retrievals from a shipboard radiometry system are comparable to continuous SPM measurements taken with a flow-through system. This is important for monitoring efforts because shipboard radiometry is more feasible than flow-through systems for setup on non-research vessels.

In our spatial variability analysis, we found that different physical environmental conditions at different times of year correspond to the total overall heterogeneity of SPM in the bay. We also found that the amount of variability is different in different parts of the bay. Central Bay has the most variability, followed by South Bay and then North Bay. In addition, the shipping channel displayed consistently less variability across spatial scales than the full Bay. This is important for understanding how monitoring programs and sampling strategies in different regions of the bay are capturing variability in water quality.

Comparison of datasets

Shipboard radiometry retrievals matched in situ measurements better than retrievals from the Sentinel-2 data, for both April and June (Figure 3). The HydroRad and underway flow-through data both followed the same spatial pattern as the *in situ* measurements (Figure 2). Changes in the relationship between HydroRad retrieved SPM and validated flow-through SPM occurred on each date, notably the April matchup relationship had a slope of 2.15 rather than 1 (Figure 2). This is likely because flow-through data were taken at 2 m depth, while

shipboard retrievals are of surface concentration. Intensified stratification from high Delta inflow and switching tides could have contributed to this inconsistency between surface radiometry data and flow-through data at depth. The shipboard radiometry has comparable data to a flow-through system and is more convenient in that it could easily be set it up on small boats or commercial boats already moving around SF Bay. This concept is being explored in other areas (i.e. the FOCUS project in British Columbia) and could be highly relevant in SF Bay if scientists partner with commercial vessels.

Both sources of continuous data from the boat show more variability and SPM features than point sampling. Additional features are visible in the higher resolution radiometry and flow-through datasets than the *in situ* point sampling, notably including a peak just after station 9. This feature occurs as part of a sill on the eastern side of the Carquinez straight due to gravitational circulation (Schoellhamer, 2000) and extends along the west side of Grizzly Bay (Figure 6). At a larger scale, all three datasets clearly capture a regional maximum in SPM that corresponds to the location of the X2 change in salinity marker (Figure 2). This matches what has been described in previous work as the North Bay Estuary Turbidity Maximum (ETM) zone (D. H. Schoellhamer 2000) which serves as an important habitat for estuarine species and marks the transition from fresh to salt water. X2 is used as a habitat indicator because it tracks the location of the ETM and is a salinity preferred by estuarine species (2 psu).

The location of the ETM is controlled by flooding events from the Delta and tides. Flooding controls sediment supply, while tides and wind control sediment suspension (Schoellhamer 2011). Tides create oscillations in ETM location, which may explain the land- and seaward shifts in the ETM observed in our data. In April, June, and October, the ETM moved landward, seaward, and then landward again associated with a tide coming in, tide going out, and coming in again. The magnitude of the ETM somewhat corresponded to the strength of the Delta flow: April and June both had higher flow (over 66,000 cfs) and ETMs of at least 50 mg/L in the flow-through data, while October had lower flow (15,000 cfs) and an ETM of about 15 mg/L (Figure 2).

Shipboard radiometry systems like the HydroRad used in our study provide hyperspectral data. We did not explicitly use the sensor's hyperspectral capacity in this study, but calls for increasing the collection of hyperspectral data in coastal ocean systems are increasingly widespread (Muller-Karger et al. 2018; Werdell et al. 2018). Consistent hyperspectral data sources could expand biological monitoring in SF Bay and improve our understanding of chlorophyll spatial variability and phytoplankton functional types (Mouw et al. 2017; Muller-Karger et al. 2018). At minimum, collecting shipboard radiometry provides hyperspectral data with no atmospheric influence at ~100 m resolution that could be used for calibration and validation of future hyperspectral sensors like PACE and SBG. Although this study largely overlooks the advantages of having a hyperspectral data source, other studies have demonstrated the potential for retrieving multiple

water quality variables from hyperspectral data (Fichot et al. 2018, Jensen et al. 2019). Using hyperspectral data may help retrieve chlorophyll-a and phytoplankton type information, which would be particularly helpful for ongoing monitoring of chlorophyll-a and other biological variables in SF Bay. Standard chlorophyll-a algorithms (like OCx) are not developed for high-sediment waters. Limited preliminary analysis of Sentinel C2RCC chlorophyll-a retrievals and Shipboard Radiometry Fluorescent Line Height products were conducted, but match-ups varied widely across dates and space. Some success has been had with retrieving chlorophyll-a in SF Bay with empirical PLSR methods (Fichot et al. 2016; Jensen et al. 2019), but they aren't reliably portable across days/locations, and the overall accuracy was estimated to be around 60% (Fichot et al. 2016).

Despite the many potential advantages to shipboard remote sensing, one major disadvantage is that it can only record data along a line. High resolution satellite imagery like that from Sentinel-2 provides significantly more spatial context than one-dimensional transect data. High spatial resolution helps resolve features in SF Bay, and is more important than spectral resolution for monitoring SPM variability. Satellite imagery has inherently more uncertainty, primarily from atmospheric effects, making it overall less accurate than ship-board monitoring. However, for monitoring highly accessible optical components like sediments, satellite imagery works well. We encourage the scientific community to continue exploring the application of shipboard radiometry as a hyperspectral data source unaffected by atmospheric interference.

Atmospheric effects might influence variability results in our Sentinel-2 SPM images. Nazirova et al. (2021) obtained the most accurate retrievals with C2RCC in a different estuary system, but observed some spatial heterogeneity in C2RCC results that were not apparent in other results from other algorithms (i.e. Nechad et al. 2010). In our data processing, we observed features in the standard Level-2A reflectance product that were not present in the shipboard ground-truth datasets. Overall, our C2RCC results matched best with *in situ* measurements, both in terms of reflectance data (Figure 3) and SPM retrievals (Figure 4).

Spatial Variability Analysis

In the spatial variability analysis, we examined the amount of spatial variability at different scales in SF Bay using the Sentinel-2 data. Satellite imagery provides context and a detailed picture of spatial patterns on each date, in different regions, and between the full bay and just within the shipping channel (Figure 6). We discuss the differences between dates, between regions, and in the shipping channel below.

Differences Between Dates

Changes in the CV/GSD relationships between dates corresponded to changes in environmental conditions. Seasonal changes in Delta flow and wind speed in combination with different tidal phase are well-known to influence SPM variability (Powell et al. 1989, Downing-Kunz et al. 2021), and influence GSD_T

and CVs across scales. The high variability in April corresponded to the highest amount of Delta inflow of any of the three dates examined. Although April and June had very similar levels of flow, April 25 was during a period of quickly declining Delta flow. In contrast, June 4 was a local peak in Delta flow. Similarly, April 25 occurred just before a spring tide, while June 4 occurred at the height of a strong spring tide. These factors point to the system being broadly in more of a transitional state in April than it was in June. In addition, the April image was taken during a high tide of 5.26 ft, and the June image was taken at a falling tide of 1.8 ft. Changes in tidal height between images account for significant differences in spatial distribution of turbidity and SPM (Fichot et al. 2016).

The influence of wind-driven resuspension is also extremely important when considering SPM spatial distribution (Bever et al. 2018), and it should be noted that April had higher winds than June. Wind direction is also important (Bever et al. 2018) and was not recorded, so more data would need to be examined to draw specific conclusions about the effects of wind on the dates we examined. Overall, it seems there were more environmental conditions in flux during April than in June, which explains the difference in variability metrics between the two dates despite them having similar Delta flow states. October was notably different from the April and June dates. Delta flow decreased by a factor of 4 to 15,000 cfs, and the tidal phase was entering neap tide. As consequence, the system was relaxing and had significantly lower SPM overall, as well as less spatial variability. These

seasonal changes in variability are likely manifestations of seasonal changes in physical environmental conditions.

We only consider three dates from 2019, and do not have data covering a long time series. Conditions in SF Bay can change dramatically year to year: for example, Delta flow throughout 2020 was much more similar to flow in October 2019 than April or June 2019. Future research should examine spatial structure and variability during more tidal states, Delta flow conditions and more extensive wind data. We recommend using a Principal Component Analysis or similar method to observe spatial variability through time, and to identify the regions of high and low SPM variability.

Differences Between the Shipping Channel and Full Bay

In the full bay vs. shipping channel analysis, the variability of the entire bay was consistently higher than the variability observed in the shipping channel (Figure 6a,6c,6e). Results show there is twice as much variability when considering the full bay compared to just the shipping channel transect. Our results suggest that data taken just within the shipping channel will underestimate the variability than exists in the full bay. This can be attributed to two things: first, the shipping channel is a distinctive region from the rest of the bay: it is potentially more homogeneous than the rest of SF Bay because it is consistently deeper (Figure 1) and experiences less wind-driven resuspension of SPM (Bever et al. 2018). Second, the data in the shipping channel were extracted along a

transect and are therefore one-dimensional while the full area dataset is two-dimensional. This is important because variability in SF Bay is not isotropic. Previous studies that have looked at spatial variability in the cross-channel direction (Fichot et al. 2016, Ruhl et al. 2001, Powell et al. 1989) confirm that spatial variability in SF Bay is anisotropic, with more heterogeneity in cross-channel datasets than within-channel datasets.

Our CV/GSD analysis assumes isotropic conditions in the Bay and overlooks the longitudinal anisotropy that exists because of the shipping channel's distinctiveness. Anisotropy could be examined more effectively using a different spatial variability analysis, such as a semi-variogram method that considers the North-South anisotropy introduced by the shipping channel. This can be done by including the direction of strongest correlation, and the anisotropy ratio which conceptually quantifies how far from isotropic the situation is.

Despite its limitations, the CV/GSD analysis does effectively illustrate the potential issues with monitoring the Bay only along the shipping channel transect: the channel is physically distinctive and sometimes less heterogeneous than the full bay. Integrating satellite image processing with current monitoring methods would not only provide spatially resolved information, but also context on cross-channel variability that is not regularly tracked.

Differences Between Regions

The results from the CV/GSD relationships between regions show that North Bay has consistently less spatial heterogeneity than Central and South Bay (Figure 6b,d,f), represented by a lower GSD_T for North Bay compared to the other regions. This is initially counterintuitive because North Bay is often thought of as highly dynamic compared to South Bay: water residence times in North Bay are about 2 weeks, compared to South Bay water residence times of about 3-5 months (Conomos 1979). However, this relatively low heterogeneity matches what is seen in the satellite imagery. For example, if we consider April as a case example: the GSD_T of North Bay is 621 m compared to 1.7 km and 1.2 km for Central and South Bay, respectively. Looking at the SPM map for that day, we see that the main source of variation in North Bay is the distinctive shipping channel. However, most of the North Bay region falls within the smaller range of SPM = 60-145 mg/L, whereas both Central and South Bay have a larger range of SPM = ~30-145 mg/L. Central and South Bay also don't have just one single distinctive feature the way North Bay does—instead, there is more widespread heterogeneity across the full area of each region, driving up the GSD_T. The strong influence of Delta flow in North Bay results in dynamic movement, but steady spatial structure. In contrast, Central and South Bay water movement is less controlled by Delta flow and instead primarily correlated to tidal phase (Cloern et al. 1989, Tobler 1970), which sets up less consistent structure and results in higher spatial variability. South Bay CV/GSD has a lower slope than other regions, which is

especially apparent in the transect data. This implies variability is being gained more slowly (less sub-1km) variability than other regions.

Implications for Monitoring

Monitoring at different resolutions in different parts of SF Bay could be informed by this analysis. Like results from other coastal areas (Moses et al. 2016), high variability at sub-kilometer scales is observed in SF Bay. The highly dynamic nature of the SF Bay estuary system essentially means that there is no point at which spatial structure becomes uniform. Therefore, monitoring decisions about sampling resolution and strategy should be made on a case-by-case basis, based on what processes are being examined and when and where the monitoring is occurring.

We make several recommendations for general sampling based on our results. First and foremost, we emphasize that recognizing the lack of variability captured in the shipping channel is important. Spatial variability in SF Bay is not isotropic, and the spatial structure of the shipping channel is not necessarily representative of the spatial variability in the rest of SF Bay. Considering data taken at dispersed stations throughout the area of SF Bay is important for any research looking to assess water quality changes or changes in SF Bay conditions. Reliance on point measurements or transect data taken solely in the shipping channel increases the likelihood of missing important outflow events or seeing peaks that are part of a larger feature or small filament.

Similarly, monitoring in different areas of SF Bay should consider the scales at which processes occur, and consider how much inherent uncertainty is incorporated with monitoring at different resolutions. For example, using the CV/GSD relationship established for April, Central Bay 10% variability (CV = 0.1) at 20 m resolution compared to 10% uncertainty in North Bay at 190m resolution. This information, in combination with using satellite imagery to identify unique and distinct features, provides a targeted view of SF Bay and context for monitoring at different times of year, different tidal states and different Delta conditions.

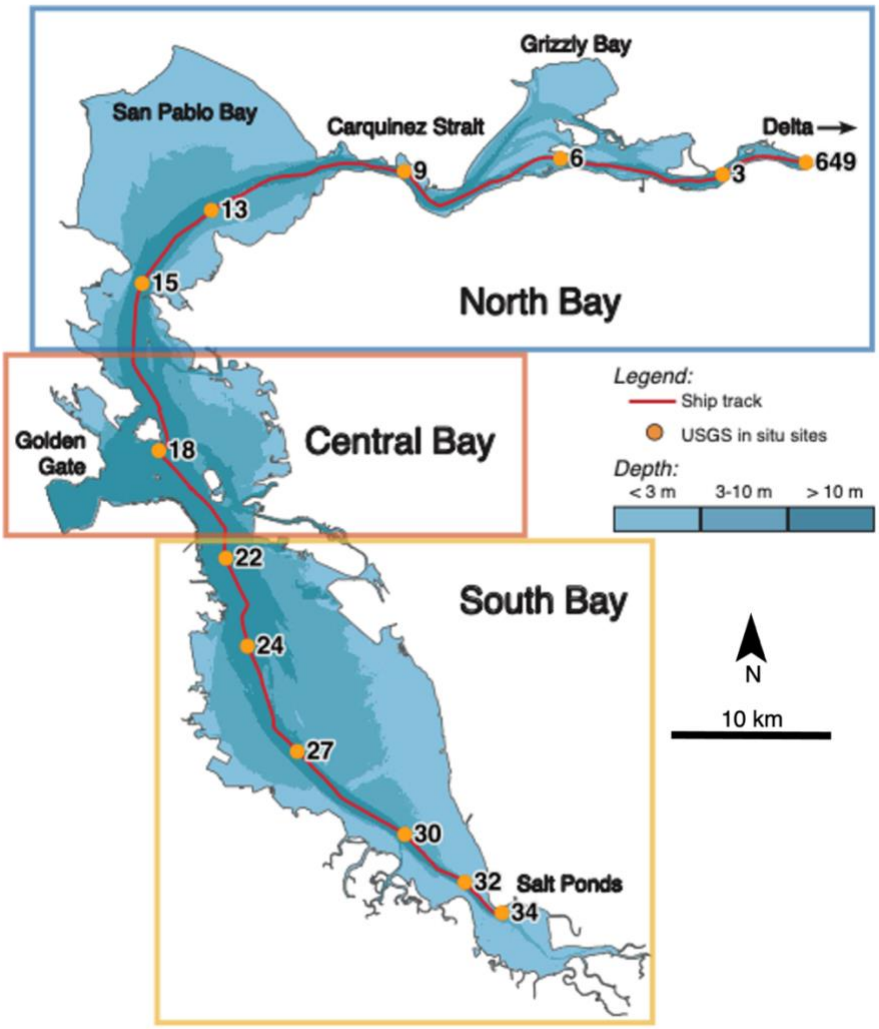

Fig. 1. Map of San Francisco Bay showing bathymetry, USGS cruise track and sampling stations used in this study, and the three regions of the Bay (North, Central, South). Flow-through data and Shipboard Radiometry were collected continuously along the ship track (red line). Radiometry average distance between samples is ~120m, Flowthrough is ~30m. Total Suspended Particulate Matter samples were collected at USGS stations (orange dots) at 2m depth.

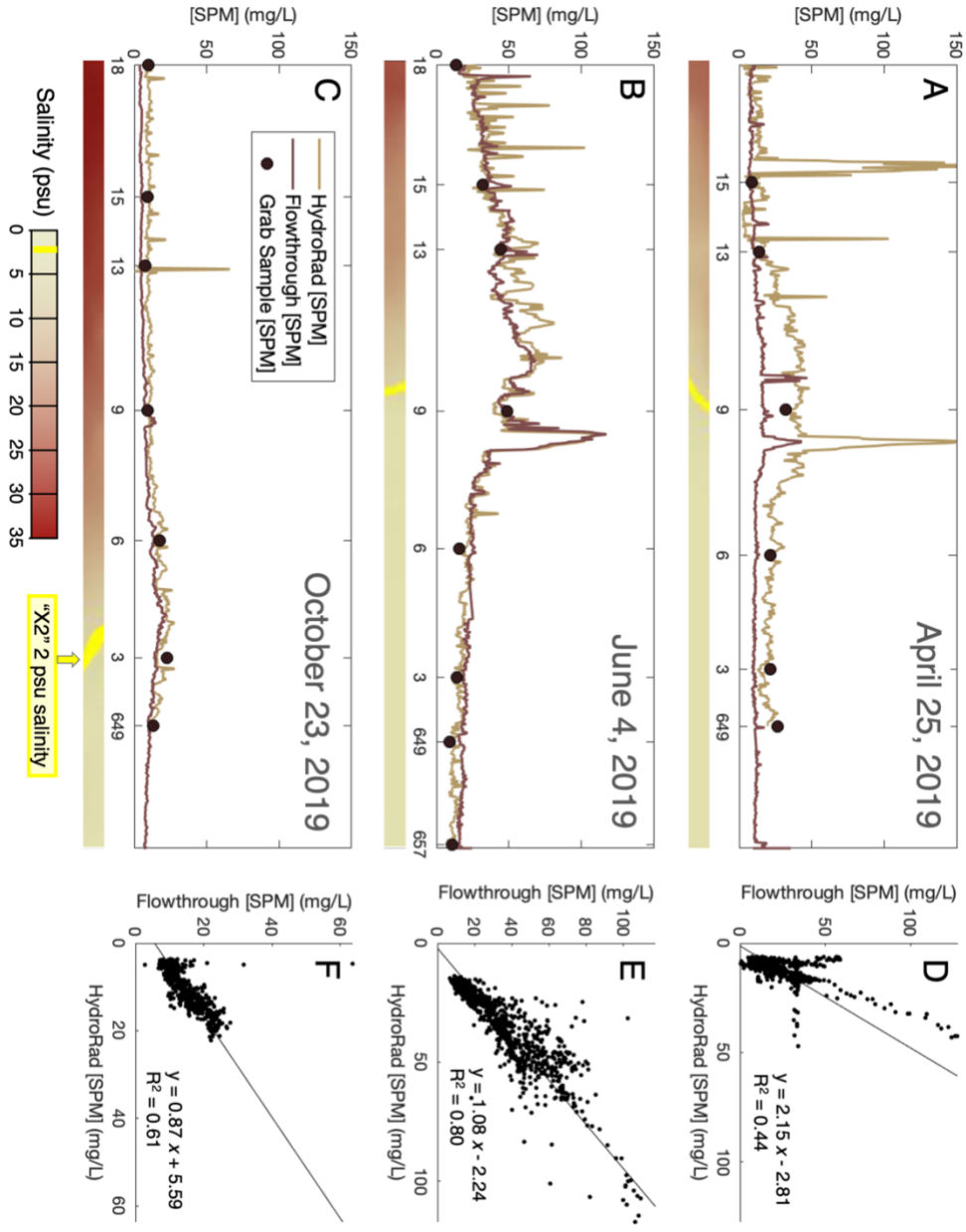

Fig. 2. SPM concentration measured by in situ grab samples, validated SCUFA flowthrough, and retrieved by the HydroRad along the cruise transect for A) April, B) June, and C) October. Transects start at USGS station 18 in Central Bay and end at station 657 near the mouth of the Delta. The x-axis is USGS station number. D, E, and F show match-ups between HydroRad retrievals and Flowthrough SPM.

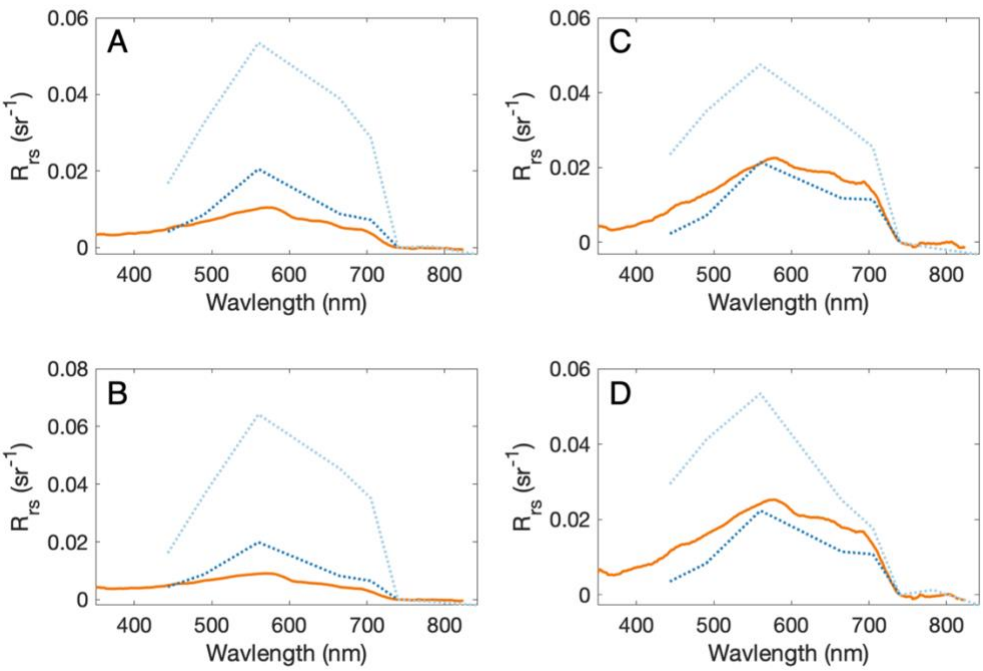

Fig. 3. Radiometric comparison of Remote Sensing Reflectance (R_{rs}) from the HydroRad at the surface (orange line), Sentinel-2 processed to Level 2A with the standard ESA correction (light blue dotted line), and Sentinel-2 reflectance processed from Level 1C using C2RCC. The comparisons shown are taken at the closest stations visited to the time of the Sentinel-2 overpass. For April, this was stations 15 and 13 (panels A and C). For June, this was stations 13 and 9 (panels B and D).

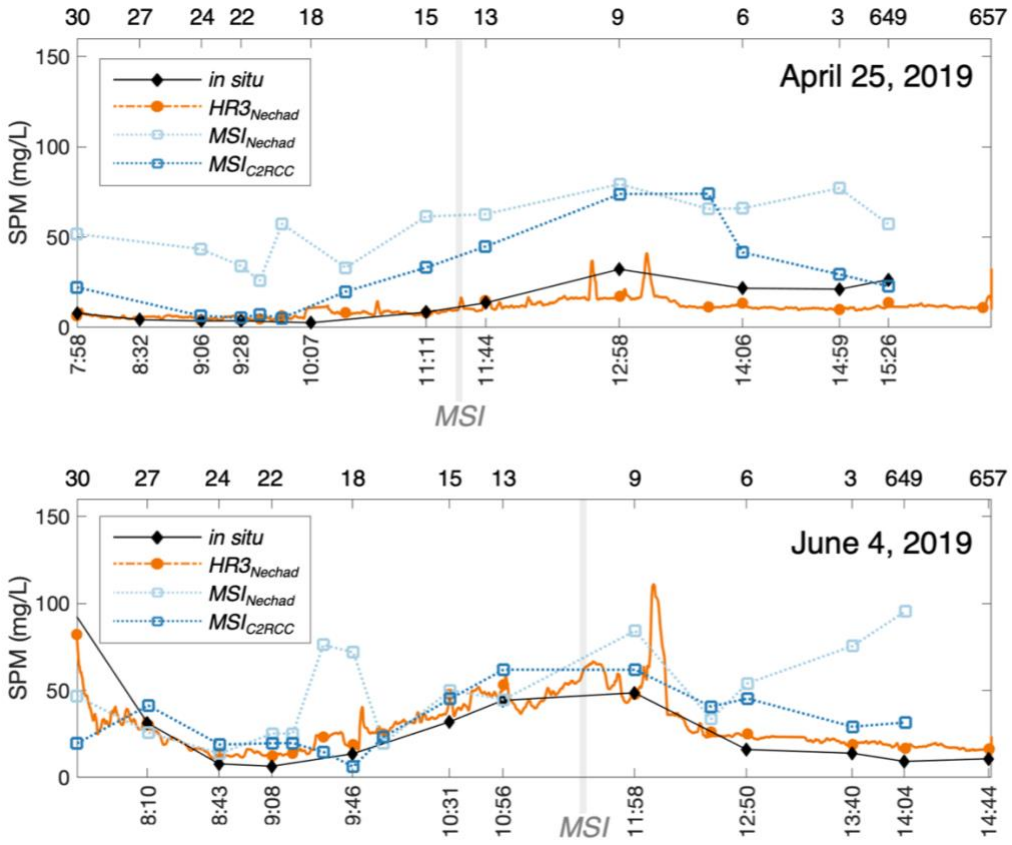

Fig. 4. SPM retrievals through SFB from the HydroRad using the Nechad et al. (2010) algorithm (solid orange line), Sentinel 2 L2A data using the Nechad algorithm (dashed light blue line), and Sentinel 2 L1C processed with CR2CC (dashed dark blue line), compared to *in situ* grab samples (black). The top axis for each panel is USGS station from station 30 (South Bay) to station 657 (mouth of Delta). The bottom axis is the time that the *R/V Peterson* was at each station. The vertical light grey line shows the time that Sentinel 2 imagery was taken.

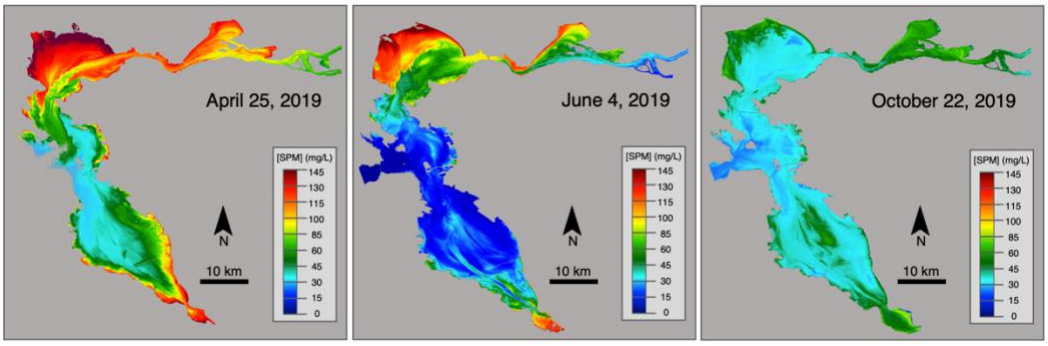

Fig. 5. SPM images generated from Sentinel-2 for each cruise date. Note the significantly higher SPM in April and June than October. In April and June, Delta flow was about 66,000 cfs, while in October Delta flow decreased to around 15,000 cfs.

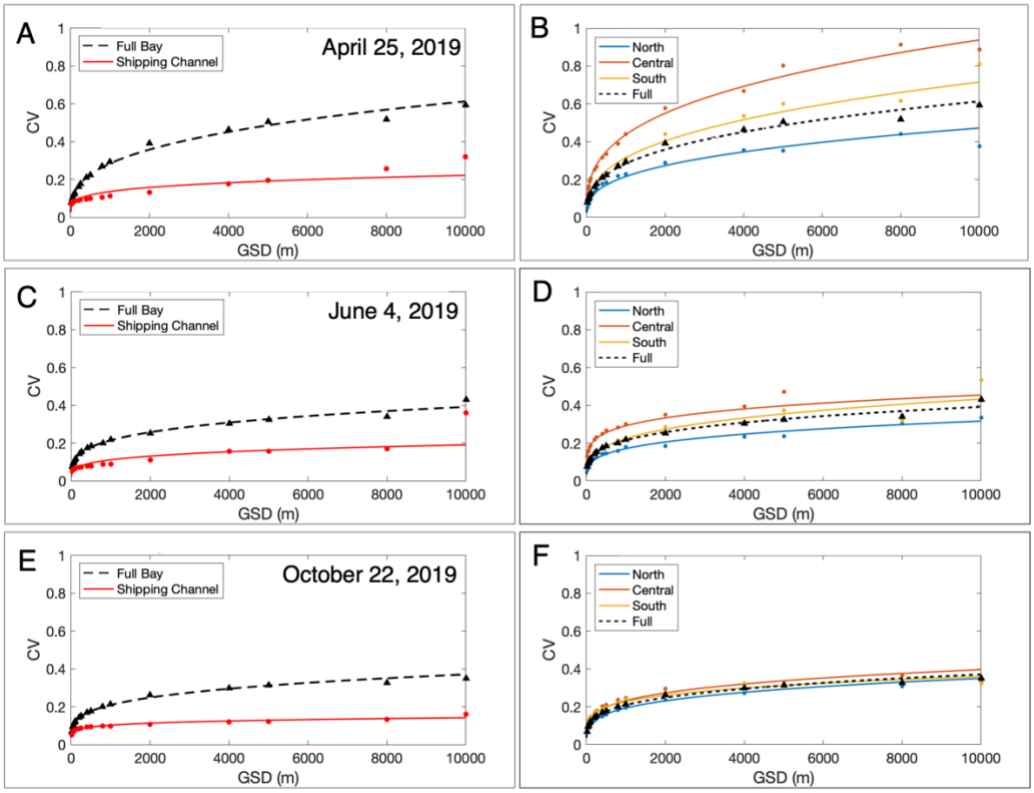

Fig. 6. Spatial variability (CV/GSD) relationships for the full San Francisco Bay on each date (black dashed lines). The left panels (A,C,E) show the CV/GSD relationship for the shipping channel. Right panels (B,D,F) show the CV/GSD relationships for each of the regions mapped in Figure 1.

	April	June	October
Min [SPM]	3	0.011	0.5
Max [SPM]	152.58	148.84	46.71
Mean [SPM]	46.25	47.78	9.06
Std [SPM]	44.94	36.13	4.94
Median [SPM]	24.99	32.46	7.11
Delta Flow (cfs)	68,464	66,005	15,845
Tidal Height (ft)	5.26	1.8	1.8
Wind speed (m/s)	7.7	0.5	1.3

Table 1. Statistics from the Sentinel 2 images of SPM generated with C2RCC and environmental data for each date.

TRANSECTS

Region	April	June	October	Average
North	140 m	110 m	100 m	116.67
Central	210 m	130 m	70 m	136.67
South	230 m	180 m	110 m	173.33
Full	210 m	170 m	100 m	160.00

AREAS

Region	April	June	October	Average
North	620 m	340 m	390 m	450.00
Central	1740 m	490 m	450 m	893.33
South	1190 m	530 m	371 m	697.00
Full	920 m	460 m	420 m	600.00

Table 2. Transition GSDs (GSD_T) for each region on each date, calculated for just the shipping channel transect (top panel) and for the full area of the region (bottom panel).

REFERENCES

Bever, Aaron J., and Michael L. MacWilliams. 2013. “Simulating Sediment Transport Processes in San Pablo Bay Using Coupled Hydrodynamic, Wave, and Sediment Transport Models.” *Marine Geology* 345: 235–53. https://doi.org/10.1016/j.margeo.2013.06.012.

Bever, Aaron J., Michael L. MacWilliams, and David K. Fullerton. 2018. “Influence of an Observed Decadal Decline in Wind Speed on Turbidity in the San Francisco Estuary.” *Estuaries and Coasts* 41 (7): 1943–67. https://doi.org/10.1007/s12237-018-0403-x.

Brockmann, Carsten, Roland Doerffer, Marco Peters, Kerstin Stelzer, Sabine Embacher, and Ana Ruescas. 2016. "Evolution of the C2RCC Neural Network for Sentinel 2 and 3 for the Retrieval of Ocean Colour Products in Normal and Extreme Optically Complex Waters.” *Celal Bayar Üniversitesi Sosyal Bilimler Dergisi* 12 (1): 1–7. http://dx.doi.org/10.1186.

Cloern, James E., and Richard Dufford. 2005. “Phytoplankton Community Ecology: Principles Applied in San Francisco Bay.” *Marine Ecology Progress Series*. https://doi.org/10.3354/meps285011.

Cloern, James E., Thomas M. Powell, and Linda M. Huzzey. 1989. “Spatial and Temporal Variability in South San Francisco Bay (USA). II. Temporal Changes in Salinity, Suspended Sediments, and Phytoplankton Biomass and Productivity over Tidal Time Scales.” *Estuarine, Coastal and Shelf Science* 28 (6): 599–613. https://doi.org/10.1016/0272-7714(89)90049-8.

Conomos, T. J., R. E. Smith, and J. W. Gartner. 1985. “Environmental Setting of San Francisco Bay.” *Hydrobiologia* 129 (1): 1–12. https://doi.org/10.1007/BF00048684.

Davis, Curtiss O. 1982. “The San Francisco Bay Ecosystem - A Retrospective Overview.” In *San Francisco Bay Use and Protection*, edited by William J. Kockelman, T. John Conomos, and Alan E. Leviton, 17–37. Pacific Division: American Association for the Advancement of Science.

Downing-Kunz, Maureen A., Paul A. Work, and David H. Schoellhamer. 2021. “Correction to: Tidal Asymmetry in Ocean-Boundary Flux and In-Estuary Trapping of Suspended Sediment Following Watershed Storms: San Francisco Estuary, California, USA (Estuaries and Coasts, (2021), 10.1007/S12237-021-00929-Y).” *Estuaries and Coasts*, no. 2005. https://doi.org/10.1007/s12237-021-00937-y.

Fichot, Cédric G., Bryan D. Downing, Brian A. Bergamaschi, Lisamarie Windham-Myers, Mark Marvin-Dipasquale, David R. Thompson, and Michelle M. Gierach. 2016. “High-Resolution Remote Sensing of Water Quality in the San Francisco Bay-Delta Estuary.” *Environmental Science and*

Technology 50 (2): 573–83. https://doi.org/10.1021/acs.est.5b03518.

Ganju, Neil K., David H. Schoellhamer, John C. Warner, Michael F. Barad, and S. Geoffrey Schladow. 2004. "Tidal Oscillation of Sediment between a River and a Bay: A Conceptual Model." *Estuarine, Coastal and Shelf Science* 60 (1): 81–90. https://doi.org/10.1016/j.ecss.2003.11.020.

Hilton, Annette E., Jesse T. Bausell, and Raphael M. Kudela. 2018. "Quantification of Polychlorinated Biphenyl (PCB) Concentration in San Francisco Bay Using Satellite Imagery." *Remote Sensing* 10 (7): 1–18. https://doi.org/10.3390/rs10071110.

Jassby, A. D., B. E. Cole, and J. E. Cloern. 1997. "The Design of Sampling Transects for Characterizing Water Quality in Estuaries." *Estuarine, Coastal and Shelf Science* 45 (3): 285–302. https://doi.org/10.1006/ecss.1996.0199.

Jensen, Daniel, Marc Simard, Kyle Cavanaugh, Yongwei Sheng, Cédric G. Fichot, Tamlin Pavelsky, and Robert Twilley. 2019. "Improving the Transferability of Suspended Solid Estimation in Wetland and Deltaic Waters with an Empirical Hyperspectral Approach." *Remote Sensing* 11 (13): 1629. https://doi.org/10.3390/rs11131629.

Mobley, Curtis D. 1999. "Estimation of the Remote-Sensing Reflectance from above-Surface Measurements." *Applied Optics* 38 (36): 7442. https://doi.org/10.1364/AO.38.007442.

Morgan-King, Tara L., and David H. Schoellhamer. 2013. "Suspended-Sediment Flux and Retention in a Backwater Tidal Slough Complex near the Landward Boundary of an Estuary." *Estuaries and Coasts* 36 (2): 300–318. https://doi.org/10.1007/s12237-012-9574-z.

Moses, Wesley J., Ackleson Steven G., Johnathan W. Hair, Chris A. Hostetler, and W. David Miller. 2016. "Spatial Scales of Optical Variability in the Coastal Ocean: Implications for Remote Sensing and in Situ Sampling." *Journal of Geophysical Research: Oceans* 121 (6): 1–15. https://doi.org/10.1002/2016JC011767.Received.

Mouw, Colleen B., Nick J. Hardman-Mountford, Séverine Alvain, Astrid Bracher, Robert J. W. Brewin, Annick Bricaud, Aurea M. Ciotti, et al. 2017. "A Consumer's Guide to Satellite Remote Sensing of Multiple Phytoplankton Groups in the Global Ocean." *Frontiers in Marine Science* 4 (February). https://doi.org/10.3389/fmars.2017.00041.

Muller-Karger, Frank E., Erin Hestir, Christiana Ade, Kevin Turpie, Dar A. Roberts, David Siegel, Robert J. Miller, et al. 2018. "Satellite Sensor Requirements for Monitoring Essential Biodiversity Variables of Coastal Ecosystems." *Ecological Applications* 28 (3): 749–60. https://doi.org/10.1002/eap.1682.

Nazirova, Ksenia, Yana Alferyeva, Olga Lavrova, Yuri Shur, Dmitry Soloviev,

Tatiana Bocharova, and Alexey Strochkov. 2021. “Comparison of in Situ and Remote-Sensing Methods to Determine Turbidity and Concentration of Suspended Matter in the Estuary Zone of the Mzymta River, Black Sea.” *Remote Sensing* 13 (1): 1–29. https://doi.org/10.3390/rs13010143.

Nechad, B., K. G. Ruddick, and Y. Park. 2010. “Calibration and Validation of a Generic Multisensor Algorithm for Mapping of Total Suspended Matter in Turbid Waters.” *Remote Sensing of Environment* 114 (4): 854–66. https://doi.org/10.1016/j.rse.2009.11.022.

Raimonet, Mélanie, and James E. Cloern. 2017. “Estuary–Ocean Connectivity: Fast Physics, Slow Biology.” *Global Change Biology* 23 (6): 2345–57. https://doi.org/10.1111/gcb.13546.

Ruhl, C. A., D. H. Schoellhamer, R. P. Stumpf, and C. L. Lindsay. 2001. “Combined Use of Remote Sensing and Continuous Monitoring to Analyse the Variability of Suspended-Sediment Concentrations in San Francisco Bay, California.” *Estuarine, Coastal and Shelf Science* 53 (6): 801–12. https://doi.org/10.1006/ecss.2000.0730.

Schoellhamer, D. H. 2000. “Influence of Salinity, Bottom Topography, and Tides on Locations of Estuarine Turbidity Maxima in Northern San Francisco Bay.” *Proceedings in Marine Science* 3 (C): 343–57. https://doi.org/10.1016/S1568-2692(00)80130-8.

Schoellhamer, David H. 2011. “Sudden Clearing of Estuarine Waters upon Crossing the Threshold from Transport to Supply Regulation of Sediment Transport as an Erodible Sediment Pool Is Depleted: San Francisco Bay, 1999.” *Estuaries and Coasts* 34 (5): 885–99. https://doi.org/10.1007/s12237-011-9382-x.

Schraga, T.S., E.S. Nejad, C.A. Martin, and J.E. Cloern. 2018. “USGS Measurements of Water Quality in San Francisco Bay (CA), Beginning in 2016 (Ver. 2.0, June 2018).” Menlo Park. https://doi.org/doi.org/10.5066/F7D21WGF.

Schraga, Tara S., and James E. Cloern. 2017. “Water Quality Measurements in San Francisco Bay by the U.S. Geological Survey, 1969-2015.” *Scientific Data* 4: 1–14. https://doi.org/10.1038/sdata.2017.98.

Tobler, W. R. 1970. “A Computer Movie Simulating Urban Growth in the Detroit Region.” *Economic Geography* 46: 234. https://doi.org/10.2307/143141.

Werdell, P. Jeremy, Lachlan I.W. McKinna, Emmanuel Boss, Steven G. Ackleson, Susanne E. Craig, Watson W. Gregg, Zhongping Lee, et al. 2018. “An Overview of Approaches and Challenges for Retrieving Marine Inherent Optical Properties from Ocean Color Remote Sensing.” *Progress in Oceanography*. Elsevier Ltd. https://doi.org/10.1016/j.pocean.2018.01.001.

CHAPTER 3

CONCLUSION

Monitoring stations placed 5 km apart diagnose general water quality and keep track of changes in overall Bay health but miss multiple features and do not capture the full variability of SF Bay. Remote sensing data from satellites and from ships can supplement existing monitoring programs by providing increased resolution and broader spatial coverage. We demonstrate this by using a ship-based radiometer and three Sentinel-2 images collected within a day of each other and *in situ* measurements. The retrievals from the ship-based data were more accurate than the retrievals from the satellite data (Figure 3) and were used to track the location of the Estuary Turbidity Maximum (ETM), which is linked to other physical variables and informs on habitat conditions. Satellite imagery of SPM spatial distributions were used to understand spatial variability in different areas of SF Bay in April, June, and October—each of which was associated with very different physical environmental conditions. We found that Central Bay consistently has the most spatial variability across all scales, while North Bay has the lowest heterogeneity. In addition, we show variability in the main shipping channel of SF Bay is about half of the variability represented in the full Bay on any given date. We suggest that the strength and type of physical processes occurring in different regions of SF Bay are what account for different levels of heterogeneity, and caution that variability in SF Bay is not isotropic.